La Protein Required for Internal Ribosome Entry Site–Directed Translation Is a Potential Therapeutic Target for Hepatitis C Virus Replication

Takayoshi Shirasaki,[1,2] Masao Honda,[1,2] Hideki Mizuno,[1] Tetsuro Shimakami,[1] Hikari Okada,[1] Yoshio Sakai,[1] Seishi Murakami,[3] Takaji Wakita,[4] and Shuichi Kaneko[1]

[1]Department of Gastroenterology, [2]Department of Advanced Medical Technology, Division of Health Medicine, Graduate School of Medicine, [3]Division of Molecular Cell Signaling, Cancer Research Institute, Kanazawa University, Kanazawa, and [4]Department of Virology II, National Institute of Infectious Diseases, Tokyo, Japan

Background. Translation of the hepatitis C virus (HCV) is mediated by an internal ribosome entry site (IRES). Here, we analyzed the functional relevance of La protein for replication of HCV using an infectious HCV clone, JFH-1.

Methods. A single-nucleotide mutation from A to U was introduced at the 338th nucleotide in the stem-loop domain IV structure of HCV IRES, which stabilized stem-loop IV and abolished translation and replication of JFH-1 almost completely.

Results. During JFH-1 replication, translation initiation factors required for HCV IRES activity, including La protein, polypyrimidine tract binding protein (PTB), PSMA7, and PCBP2, were significantly induced in Huh-7.5 cells. Interestingly, JFH-1 infection increased telomerase activity and induced the expression of human telomerase RNA (hTR) in Huh-7.5 cells. In 37 tissue specimens from patients with chronic hepatitis C, La protein significantly correlated with the representative essential telomerase components hTR, p23, and HSP90 ($P < .001$). Recombinant adenovirus that expressed short-hairpin RNA against La protein successfully suppressed the levels of La protein and core protein of JFH-1 to 30% of that in the control cells.

Conclusions. HCV infection might be strongly related to telomerase activity in the liver through La protein induction. Inhibition of La protein substantially repressed JFH-1 replication; therefore, La protein is a potential therapeutic target for HCV.

Hepatitis C virus (HCV) is a positive-strand, enveloped RNA virus that belongs to the genus *Hepacivirus* in the family *Flaviviridae.* A human liver infected with HCV develops chronic hepatitis, cirrhosis, and in some instances, hepatocellular carcinoma [1]. Although a combination of ribavirin and interferon has become a routine means of treating infected patients, the results are often unsatisfactory, especially in patients with a high viral load [2]. Identification of host factors that regulate HCV replication in infected patients could be helpful in the development of a novel antiviral treatment strategy. It has been reported that various host factors are associated with HCV infection; however, only a few proteins have been functionally shown with an infectious HCV clone to regulate HCV replication [3].

The translation of HCV is initiated by a highly structured RNA segment, the internal ribosome entry site (IRES), which occupies most of the 5′ nontranslated RNA [4]. Many canonical and noncanonical translation initiation factors, such as La protein [5], polypyrimidine tract binding protein (PTB) [6], and eukaryotic initiation factor 3 (eIF3), interact with HCV IRES and might regulate HCV translation. Previously, we reported that HCV IRES activity is highly dependent on these initiation factors, and it correlated with the expression of La protein [7, 8]. However, the functional relevance of these translation initiation factors on HCV

Received 17 September 2009; accepted 6 January 2010; electronically published 24 May 2010.

Potential conflicts of interest: none reported.

Financial support: This study is partially supported by the Grants-in-Aid for Scientific Research by Japan Society for the Promotion of Science (project 17591036).

Reprints or correspondence: Dr Masao Honda, Department of Gastroenterology, Graduate School of Medicine, Kanazawa University, Takara-Machi 13-1, Kanazawa 920-8641, Japan (mhonda@m-kanazawa.jp).

The Journal of Infectious Diseases 2010;202(1):75–85

0022-1899/2010/20201-0009$15.00
DOI: 10.1086/653081

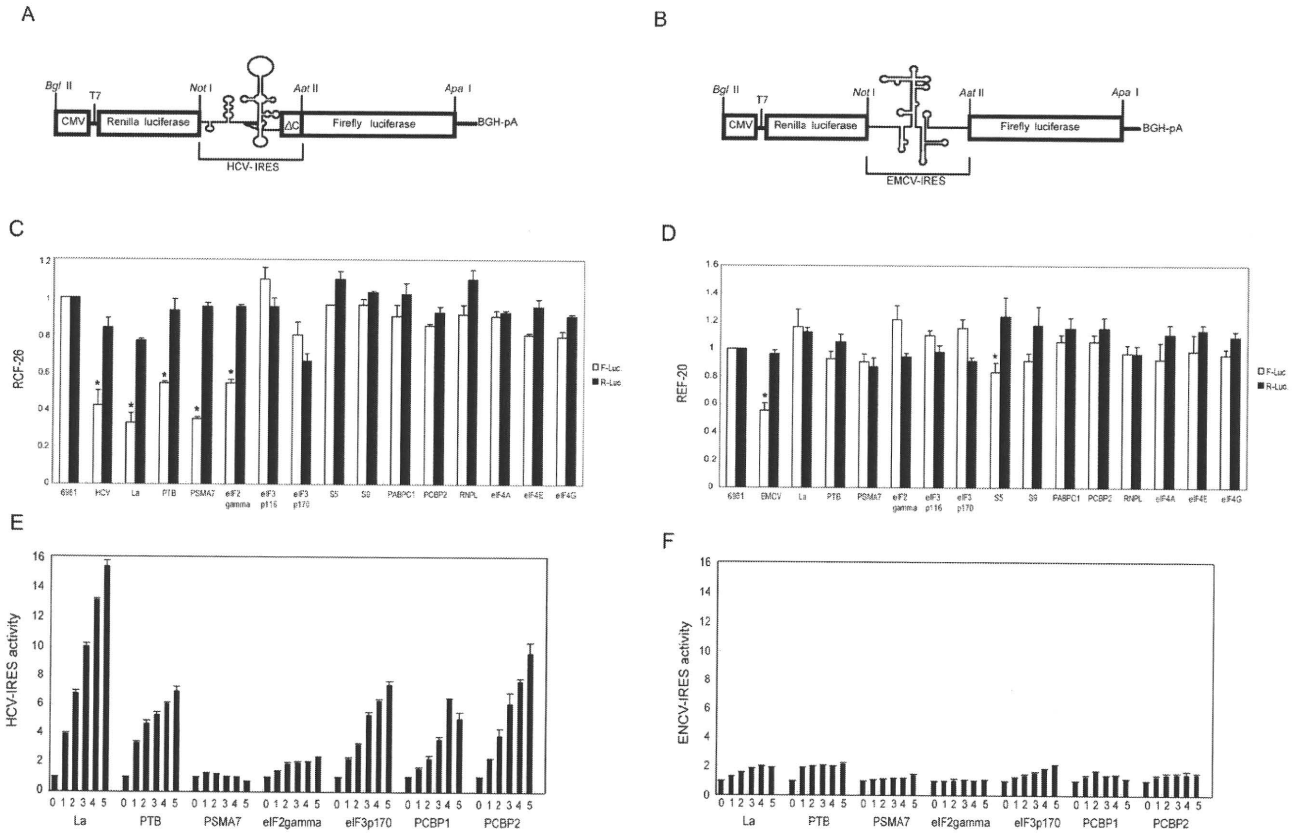

Figure 1. Organization of the transcriptional unit of plasmids pRL-HL (*A*) and pRL-EL (*B*). *C* and *D*, Suppression of 14 canonical and noncanonical initiation factors by specific antisense oligonucleotides. Changes in *Renilla* luciferase (RL) and firefly luciferase (FL) (hepatitis C virus–internal ribosome entry site [HCV-IRES]–directed translation) activities in RCF-26 (*C*). Changes in RL and FL (encephalomyocarditis virus [ENCV]–IRES–directed translation) activities in REF-20 (*D*). *$P < .05$. *E* and *F*, In vitro translation of pRL-HL and pRL-EL in rabbit reticulocyte lysate. The plasmids pRL-HL or pRL-EL (0.05 μg) and increasing amounts of expression vectors (0–0.125 μg) of La protein, polypyrimidine tract binding protein (PTB), eIF3p 170, eIF2γ, PSMA7, PCBP1, and PCBP2 were co-translated in rabbit reticulocyte lysate. The fold increases in relative HCV IRES activity (*E*) and ENCV-IRES activity (*F*) are shown. *$P < .05$. *Lane 0*, 0 μg; *lane 1*, 0.025 μg; *lane 2*, 0.05 μg; *lane 3*, 0.075 μg; *lane 4*, 0.1 μg; *lane 5*, 0.125 μg. *$P < .05$.

replication had not been fully evaluated. In this study, we found that the expression of La protein is induced by HCV infection, and this induced La protein–activated telomerase activity in a human hepatoma cell line. The results indicate La protein is a potential therapeutic target for HCV infection.

EXPERIMENTAL PROCEDURES

Expression vector plasmids. The FLAG tag fusion La protein expression vector (pCMV-La-FLAG) was created by polymerase chain reaction (PCR), using the La protein expression vector (pCMV-La) as the template [8]. The forward primer 5′-AAT GAA ATC AGA AGA AA-3′ contains an *Xba* I site, and the reverse primer 5′-TGA TCT AGA TTA CTT ATC GTC GTC ATC CTT GTA ATC CTG GTC TCC AGC ACC ATT TTC TGT TTT CTG TTG -3′ contains *Xba* I and FLAG sites.

Cell lines. Human hepatocellular carcinoma 7 (Huh-7) cells and Huh-7.5 cells (provided by Professor C. M. Rice, Rockefeller University) were maintained in Dulbecco modified Eagle medium (DMEM; Gibco BRL), which contained 10% fetal bovine serum and 1% penicillin/streptomycin. The RCF-26 was a stably transformed cell line from Huh-7 cells that constitutively expressed dicistronic RNA transcripts containing sequences encoding 2 reporter proteins—*Renilla* luciferase and firefly luciferase—separated by a functional HCV IRES of genotype 1b (Figure 1*A*) [7]. The REF-20 was a stably transformed cell line from Huh-7 cells that constitutively expressed dicistronic RNA transcripts in which HCV IRES was replaced with encephalomyocarditis virus (EMCV) IRES (Figure 1*B*).

Antisense oligodeoxynucleotide. The antisense phosphorothioate oligodeoxynucleotides (oligos) designed for HCV IRES, La protein, PTB, eIF3, eIF2γ, S9, poly(A)-binding protein cytoplasmic 1 (PABPC1), PCBP2, RNPL, and control randomized oligo 6961 were described elsewhere [8]. Antisense oligos for PSMA7, S5, eIF4A, eIF4E, eIF4G, and EMCV IRES were synthesized. The nucleotide sequences of the antisense oligos were 5′-CTC ATG CCG GCG GGC GGC CG-3′ for PSMA7,

5′-GTC ATC CTG AGA ACA CAG CC-3′ for S5, 5′-GAC ATG ATC CTT AGA AAC TA-3′ for eIF4A, 5′-GCC ATC TTA GAT CGA TCT GA-3′ for eIF4E, 5′- GAC ATG ATC TCC TCT GTG AT-3′ for eIF4G, and 5′-TCC ATA TTA TCA TCG TGT TT-3′ for EMCV IRES. The antisense oligos (1.0 μmol/L) were transfected into RCF-26 (Figure 1*C*) or REF-20 (Figure 1*D*). After 24 h of transfection, *Renilla* luciferase (cap-dependent translation) and firefly luciferase (HCV or EMCV-directed translation) activities were measured with the Dual-Luciferase Reporter Assay System (Promega).

In vitro translation of pRL-HL and pRL-EL in rabbit reticulocyte lysate. In vitro translation of pRL-HL and pRL-EL was carried out in transcription and translation–coupled rabbit reticulocyte lysate systems (Promega). In 25 μL of the transcription and translation reaction mixture, 0.05 μg of pRL-HL or pRL-EL was cotranslated with an increasing amount of plasmid DNA (up to 0.125 μg) of La, PTB, PSMA7, eIF2-γ, eIF3p170, PCBP1, and PCBP2, which were cloned using the T7 promoter. A 3-μL aliquot was then used to measure *Renilla* luciferase and firefly luciferase activities using the Dual-Luciferase Reporter Assay System (Promega).

Site-directed mutagenesis. The plasmid pJFH-1 was used as the template for introduction of the site-directed mutation at nucleotide 338 in the 5′ nontranslated RNA. The site-directed mutagenesis reaction was performed using the Pfu Turbo DNA polymerase PCR system (Stratagene), according to the manufacturer's instructions.

Transfection of JFH-1 and JFH-1 338U into Huh-7.5 cells. Ten micrograms of synthetic RNA transcribed from pJFH-1 or pJFH-1 338U was used for electroporation. Cells were then pulsed at 260 V and 950 μF using the Gene Pulser II apparatus (Bio-Rad Laboratories).

Infection of Huh-7.5 cells with JFH-1. Seventy-two hours after transfection, the culture medium was collected, cleared by low-speed centrifugation at 2000 revolutions per minute at 760g for 10 min, and passed through a Millipore filter (pore size, 0.45 μm; Millipore Corporation). Part of the filtered culture medium was diluted 50-fold or 10-fold with DMEM containing 10% fetal bovine serum and 1% penicillin-streptomycin. Diluted culture medium (1 mL) was used for injection of cells into a well of a 6-well plate or a well containing cover slips and incubated for 4 h. At 3 days after infection, inoculated cells grown on cover slips were fixed and stained using anti-core antibody, as described below. The amounts of HCV RNA, La-RNA, and human telomerase RNA (hTR)-RNA in inoculated cells were determined by quantitative real-time detection (RTD)-PCR.

Western blot analysis and immunofluorescence staining. The expression levels of La protein and PTB in cells were evaluated by Western blotting using mouse anti-La antibody (SW5) and rabbit anti-PTB antibody, as described elsewhere [9]. The expression of HCV core protein, PSMA7, eIF2γ, PCBP2, and FLAG-tagged La protein was evaluated with mouse anti-core antibody (Affinity BioReagents), mouse anti-PSMA7 antibody (Antibodies Direct), rabbit anti-eIF2γ antibody (Abcam), mouse anti-huRNP E2 (23-G) antibody (Santa Cruz Biotechnology), and mouse anti-FLAG antibody (Sigma), respectively. For immunofluorescence staining, anti–core monoclonal antibodies and Alexa Fluor 488 goat anti–mouse immunoglobulin G antibody (Invitrogen) were used.

Quantitative RTD-PCR. The primer pairs and probes for La protein, PTB, eIF3 p170, GAPDH, and HCV were obtained as described elsewhere [8]. The primer pairs and probes for PSMA7, eIF2γ, PCBP2, hTR, p23, Hps90, and β-actin were obtained from the TaqMan assay reagents library. One microgram of isolated RNA was reverse-transcribed to complementary DNA using SuperScript II RT (Invitrogen) according to the manufacturer's instructions, and the resulting complementary DNA was amplified with appropriate TaqMan assay reagents [10].

Telomerase activity assay. The plasmids pCMV-La-FLAG and pCR3.1 were transfected into Huh-7 cells using Fugene 6 transfection reagent (Roche Applied Science). Forty-eight hours after transfection, the amounts of hTR-RNA in the transfected cells were determined by RTD-PCR. The expression of the FLAG-tag fusion La protein was evaluated by Western blot analysis. Telomerase activity was measured with a PCR-based telomerase repeat amplification protocol (TRAP) assay, performed with the TRAPEZE kit (Invitrogen) according to the manufacturer's instructions. Each reaction product was amplified in the presence of a 36-base pair internal telomerase assay standard. The PCR products were fractionated by electrophoresis on a 10% polyacrylamide gel and then visualized by staining with SYBR Green (Molecular Probes).

Construction of recombinant adenovirus expressing short-hairpin RNA for La protein. The short-hairpin RNA expression plasmid (pSh-La), which expresses short-hairpin RNA for La protein (seq: 5′-CCG GCC AAG GCA GAA CTC ATG GAA ACT CGA GTT TCC ATG AGT TCT GCC TTG GTT TG-3′), was purchased from Sigma. The pSh-La was digested with the enzymes *Hin*d III and *Bam*HI, and the excised fragment, including the short-hairpin RNA, was transferred to the adenoviral expression plasmid. The adenoviral expression plasmid and bovine growth hormone plasmid were cotransfected into 293A cells using the CellPhect Transfection kit (GE Healthcare) to produce crude adenoviral stocks. These stocks were purified using the Adeno-X Virus Purification kit (Clontech Laboratories) and stored at −80°C. The titers of the adenoviral stocks were adjusted to 4.0×10^9 PFU/mL.

Twelve hours after JFH-1 RNA transfection, the cells were washed 3 times with phosphate-buffered saline, and then Ad-shLa or Ad-Null was added at a multiplicity of infection of 10.

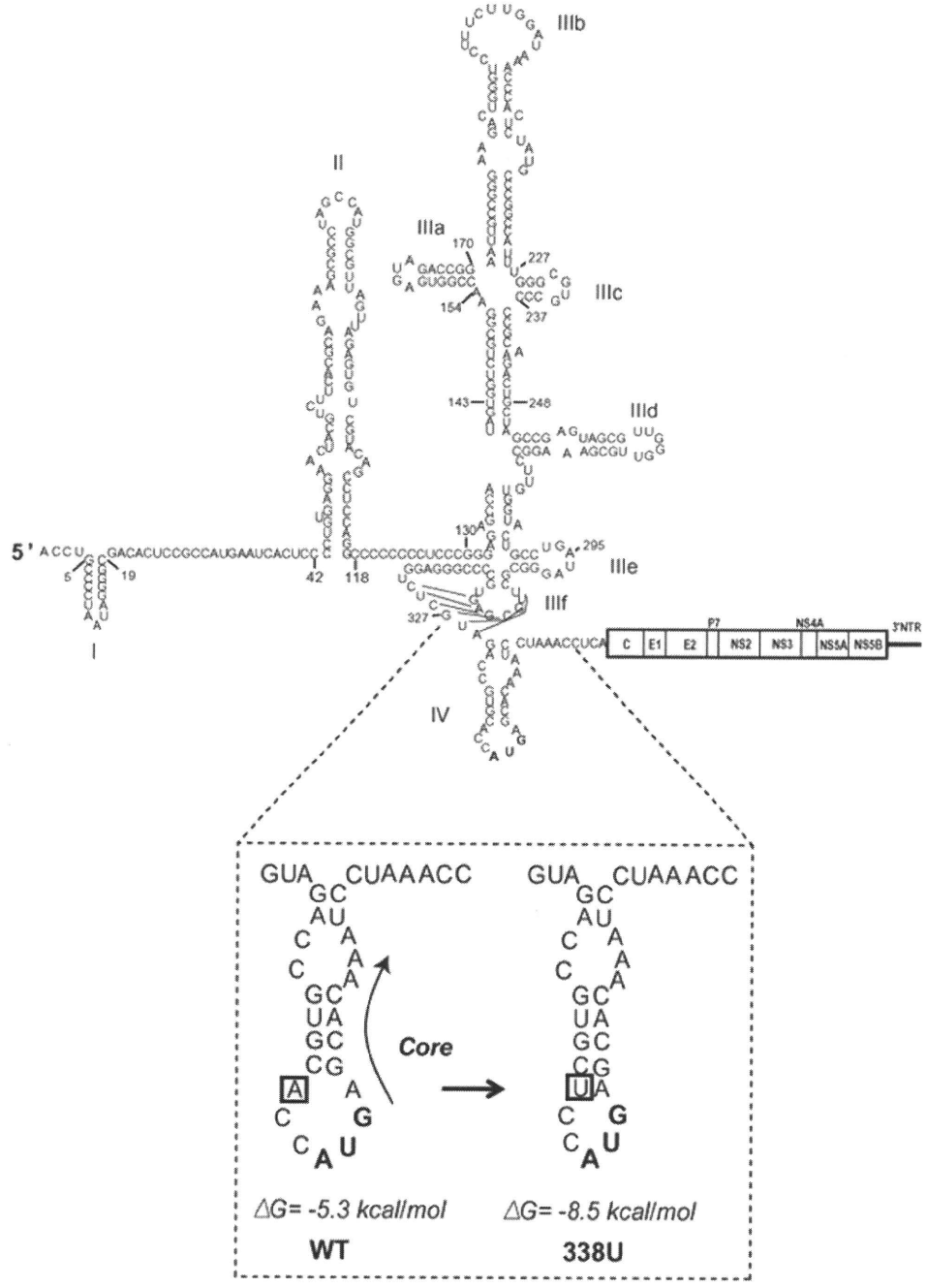

Figure 2. Organization of the full-length JFH-1 and the mutation at nucleotide 338 of stem loop IV.

One hour after injection, the cells were washed 3 times with phosphate-buffered saline, and complete culture medium was added.

Statistical analysis. Results were expressed as mean values ± standard deviation. Significance was tested by 1-way analysis of variance with Bonferroni methods, and differences were considered statistically significant at $P < .05$.

RESULTS

Dependence of HCV IRES activity on translation initiation factors. To confirm that HCV IRES activity was highly dependent on translation initiation factors, antisense oligonucleotides designed for 14 translation initiation factors were transfected into RCF-26 and REF-20 cells, and HCV or EMCV IRES

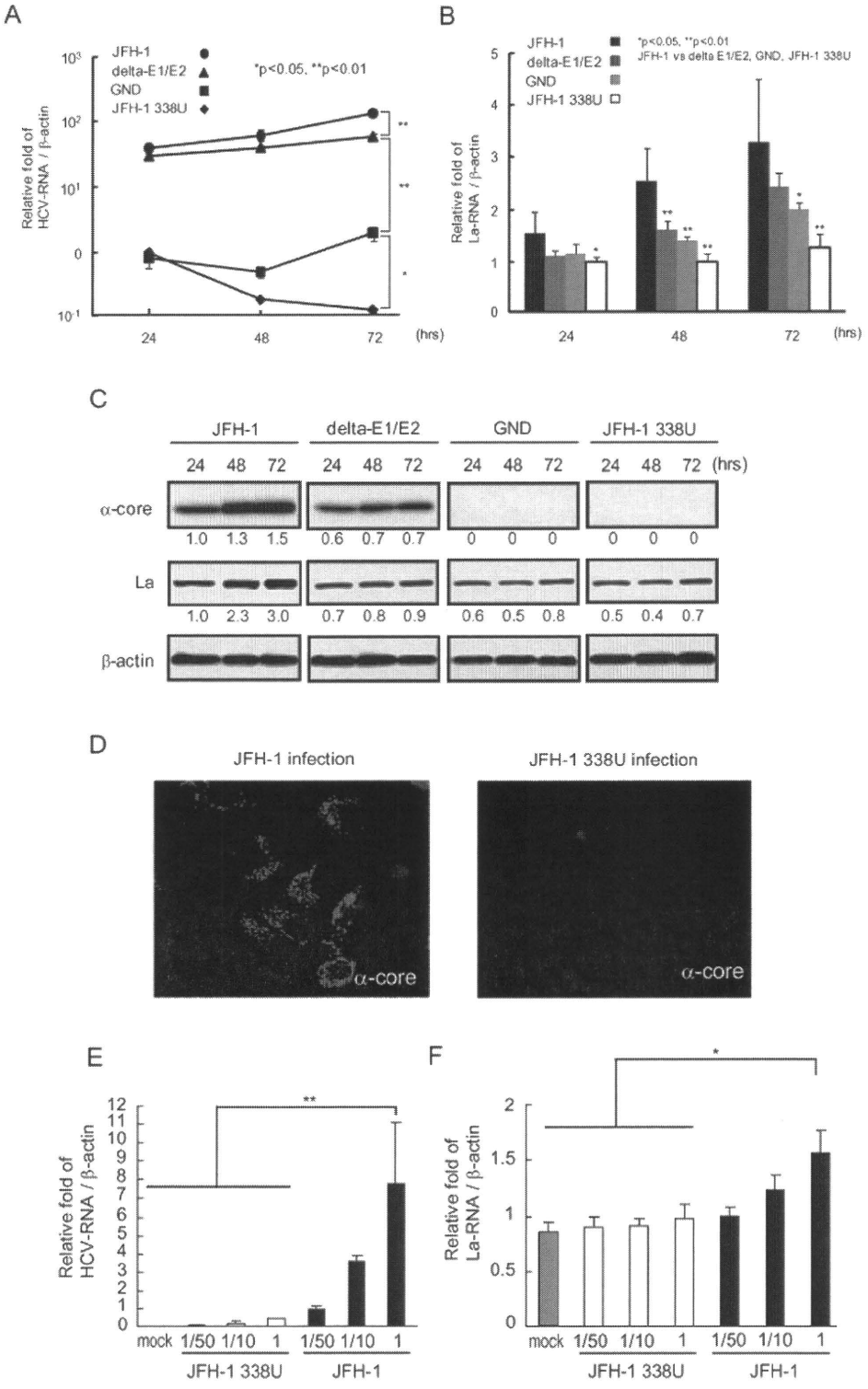

Figure 3. *A*, Hepatitis C virus (HCV) RNA replication determined by real-time detection–polymerase chain reaction (RTD-PCR) in JFH-1, JFH-1/delta E1-E2, JFH-1/GND, and JFH-1 338U transfected cells. *$P < .05$. **$P < .01$. *B*, La RNA expression determined by RTD-PCR in JFH-1, JFH-1/delta E1-E2, JFH-1/GND, and JFH-1 338U transfected cells. *$P < .05$. **$P < .01$. *C*, Western blots for detection of HCV core protein and La protein in JFH-1, JFH-1/delta E1-E2, JFH-1/GND and JFH-1 338U transfected cells. *D*, Immunofluorescence staining of core protein in Huh-7.5 cells infected with JFH-1 or JFH-1 338U. *E* and *F*, HCV RNA and La RNA determined by RTD-PCR in Huh-7.5 cells infected with serial dilution of JFH-1 or JFH-1 338U. *$P < .05$, **$P < .01$.

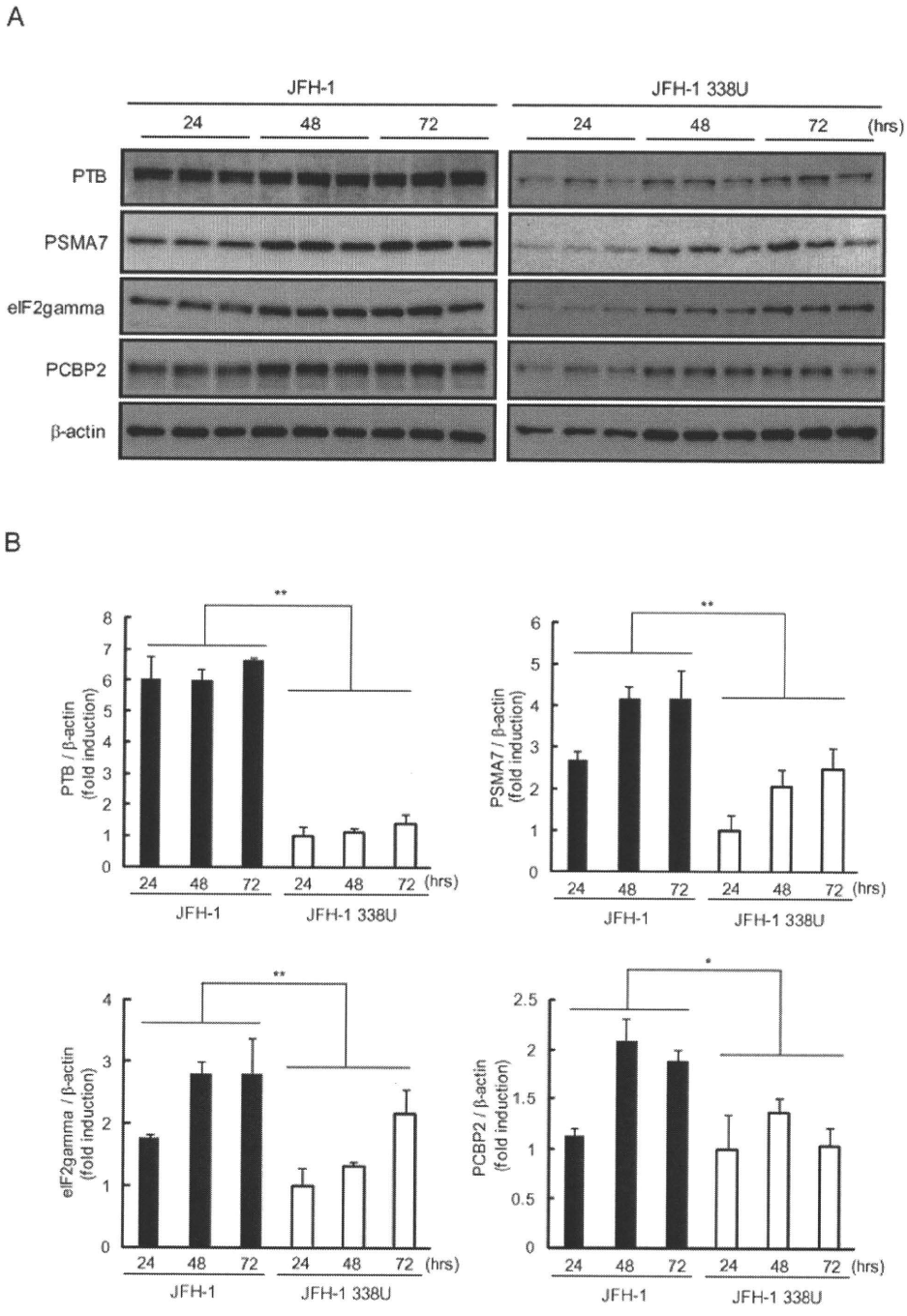

Figure 4. *A*, Protein expression of PTB, PSMA7, eIF2γ, and PCBP2 determined with Western blotting in Huh-7.5 cells after transfection with JFH-1 RNA and JFH-1 338U RNA. *B*, Quantitative densitometric analysis of protein expression. $^{*}P < .05$, $^{**}P < .01$.

activity was evaluated. The activities of *Renilla* luciferase and firefly luciferase expressed in these cells reflect cap-dependent and HCV or EMCV IRES directed translation, respectively (Figure 1*B* and 1*C*). The suppression of La protein, PTB, PSMA7, and eIF2γ by the antisense oligonucleotides in RCF-26 significantly repressed firefly luciferase activities, whereas *Renilla* luciferase activities were mostly maintained (Figure 1*C*). In contrast, these translation initiation factors did not affect EMCV IRES activity in REF-20 cells (Figure 1*D*).

These findings were also evaluated in rabbit reticulocyte lysates (RRL). With increasing amounts of expression vectors or La protein, PTB and eIF3 p170, the HCV IRES activity increased significantly (7-fold to16-fold) (Figure 1*E*). Although the depletion of PCBP2 did not affect HCV IRES activity in the RCF-

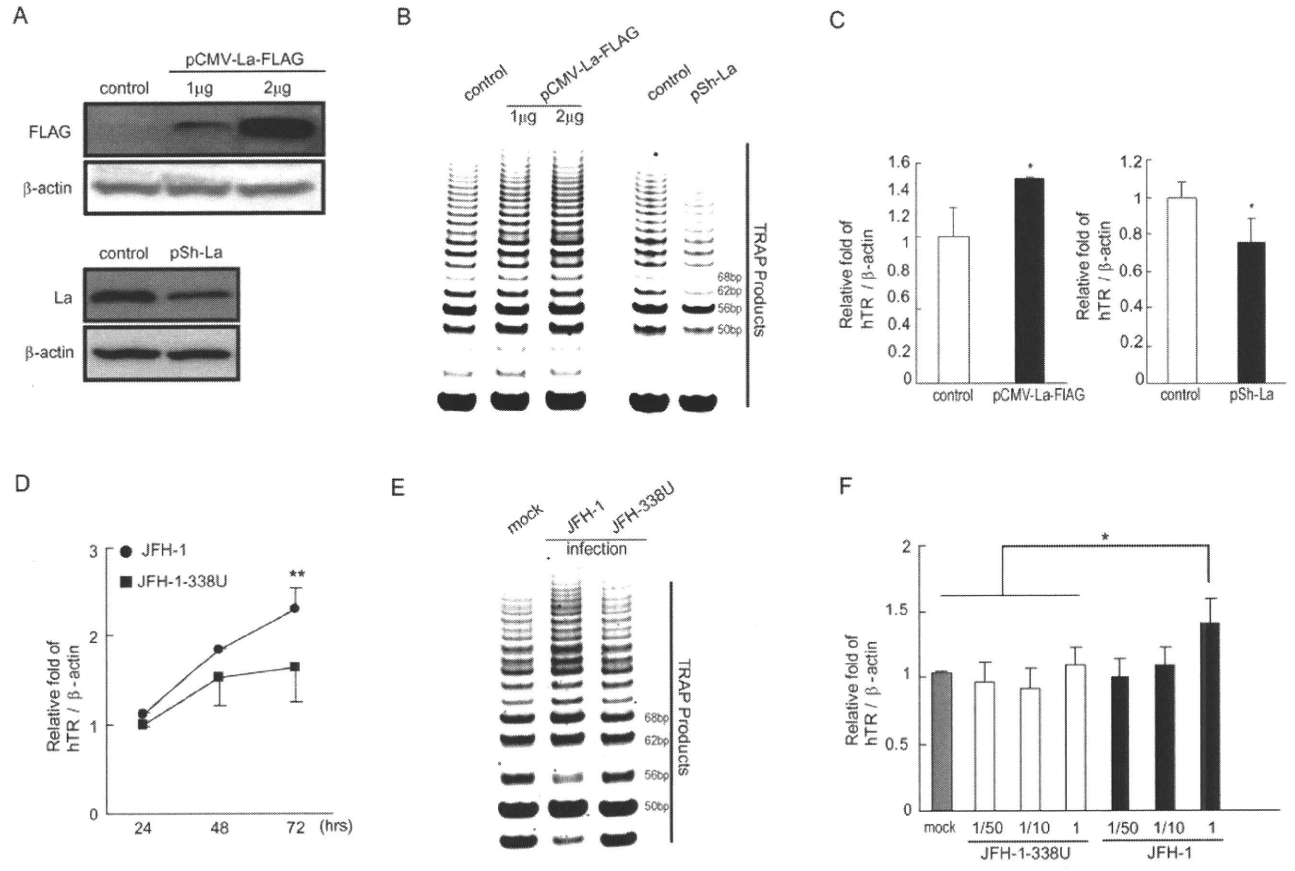

Figure 5. *A*, Western blot analysis of pCMV-La-FLAG or pSh-La transfected Huh-7 cells. *B*, The telomerase repeat amplification protocol (TRAP) assay in pCMV-La-FLAG or pSh-La transfected Huh-7 cells. *C*, Human telomerase RNA (hTR) expression in pCMV-La-FLAG or pSh-La transfected Huh-7 cells by real-time detection–polymerase chain reaction (RTD-PCR). $*P < .05$. *D*, The hTR expression in JFH-1 or JFH-1 338U RNA-transfected Huh-7.5 cells by RTD-PCR. $**P < .01$. *E*, The TRAP assay in JFH-1 or JFH-1 338U infected Huh-7 cells. *F*, Effect of JFH-1 or JFH-338U infection on hTR expression in Huh-7.5 by RTD-PCR. $*P < .05$.

26 cells, it stimulated HCV IRES activity up to 10-fold in the RRL (Figure 1*E*). On the other hand, EMCV IRES activity increased modestly by up to 2-fold (Figure 1*F*). These findings confirmed previous findings that HCV IRES activity is highly dependent on cellular factors.

Construction of translation incompetent full-length infectious HCV clone. JFH-1 is a genotype 2a-derived full length infectious HCV clone [11]. To evaluate the essential role played by IRES activity in HCV replication, we constructed a translation incompetent JFH-1 by introducing a single-nucleotide mutation from adenine to uracil at the position of nucleotide 338 (the third nucleotide upstream of the initiation codon of the core protein) in the 5′ nontranslated RNA (JFH-1 338U) (Figure 2). This mutation decreased the free energy (ΔG = 5.3 to −8.5 kcal/mol) and stabilized the folding structure of stem-loop domain IV that includes the initiation codon of the core protein. This mutation impairs ribosomal access to the AUG codon for translation initiation of viral proteins, as reported elsewhere [12].

Transfection of JFH-1 RNA into Huh-7.5 cells resulted in a substantial increase in viral RNA and core protein, as determined with RTD-PCR (Figure 3*A*), indirect immunofluorescence staining (data not shown), and Western blot analysis (Figure 3*C*). In contrast, translation-incompetent JFH-1 338U resulted in no evidence of viral replication or protein translation (as shown in Figure 3*A* and 3*C*). This indicated the functional importance of stem-loop IV not only for translation initiation but also for viral replication. Therefore, we used JFH-1 338U as an appropriate negative control in additional experiments.

Expression of La protein induced by JFH-1 in Huh-7.5 cells. Previously, we reported that expression of La protein was induced in the livers of patients with chronic hepatitis C, and the expression of La protein showed significant correlation with HCV RNA in tissue specimens from these patients [8]. In this study, we explored whether HCV might directly induce expression of La protein. The synthetic RNAs of JFH-1, JFH-1/delta E1-E2, JFH-1/GND [11], and JFH-1 338U were transfected into Huh-7.5 cells, and the expression of La RNA was

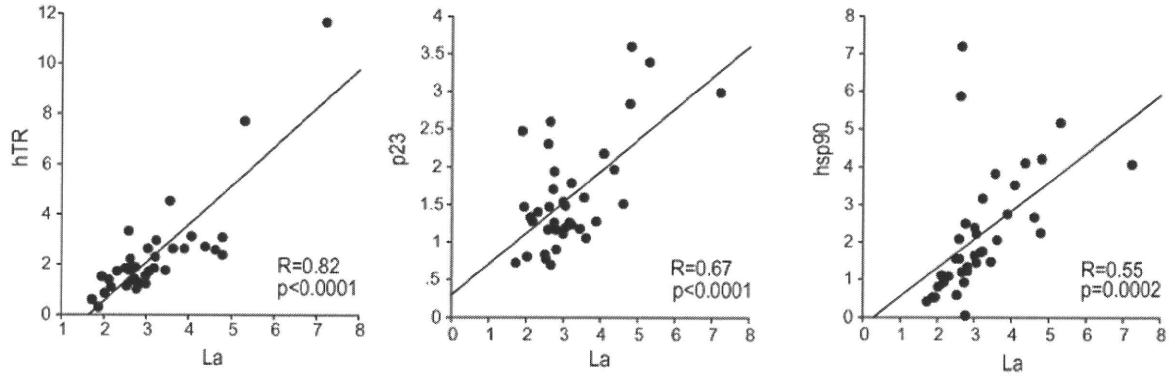

Figure 6. Correlation between expression of La protein and activity of human telomerase RNA (hTR), p23, and Hsp90 in liver biopsy specimens obtained from 37 patients with chronic hepatitis C.

evaluated after transfection by RTD-PCR and Western blot analysis. JFH-1 RNA peaked at 72 h after transfection (Figure 3*A*), as did the level of HCV core protein (Figure 3*C*). The JFH-1/delta E1-E2 RNA peak was significantly hampered compared with JFH-1 owing to the defective feature of infection. JFH-1 338U RNA and JFH-1/GND RNA was almost negligible at 72 h after transfection (Figure 3*A*) and a significant decline in JFH-1 338U RNA was noted. Under these conditions, La RNA was mostly induced in Huh-7.5 cells transfected with JFH-1, compared with JFH-1/delta E1-E2, JFH-1/GND, and JFH-1 338U (Figure 3*B*).

Similarly, expression of La protein was significantly increased after JFH-1 replication in Huh-7.5 cells, whereas only a slight increase was noticed in Huh-7.5 cells transfected with JFH-1/GND or JFH-1 338U (Figure 3*C*). The results indicated that JFH-1 replication induced La protein in Huh-7.5 cells.

To examine these findings further, the culture medium of the Huh-7.5 cells that included infectious HCV particles was collected and used to infect fresh Huh-7.5 cells at dilutions of 1:1, 1:10, and 1:50. HCV infection in the Huh-7.5 cells was confirmed by the expression of core protein (Figure 3*D*) and the presence of HCV RNA (Figure 3*E*). HCV infection was dependent on the amount of inoculated virus, as shown in Figure 3*E*. In contrast, there was no evidence of infection when using culture medium from Huh-7.5 cells transfected with JFH-1 338U RNA (Figure 3*D*, 3*E*). La RNA was significantly increased by the infection of virus derived from JFH-1 but not that derived from JFH-1 338U (Figure 3*F*). These results suggest that HCV infection itself could induce La protein in Huh-7.5 cells.

As for other initiation factors such as PTB, PSMA7, eIF2γ, and PCBP2, which were shown to be essential factors for HCV IRES activity (Figure 1), we also evaluated their gene expression according to the replication of JFH-1 (Figure 4). Western blotting of each initiation factor after JFH-1 RNA transfection showed significantly increased PTB, PSMA7, eIF2γ, and PCBP2. The increase was significantly greater in JFH-1 RNA transfected cells than in JFH-1 338U RNA transfected cells. Thus, HCV induces these initiation factors, and in turn, they served for HCV replication. Importantly, these relationships might be true in the tissue lesions of chronic hepatitis C. There were also significant correlations between the expression of these initiation factors and HCV RNA in the tissue specimens from patients with chronic hepatitis C, although the correlation between PTB, eIF3 p170, and HCV RNA was less than La protein, PSMA7, eIF2γ, PCBP2, and HCV RNA (data not shown) [8].

Activation of telomerase activity by La protein through the increase of human telomerase RNA. We next investigated the functional relevance of induced La protein in hepatocytes. Human telomerase plays an important role in cellular senescence and carcinogenesis. Human telomerase reverse transcriptase and hTR, as an RNA template, are core components of telomerase activity. In addition, other telomerase components, such as Hsp90 and p23 [13], have been reported to be essential for telomerase activity. There is a report that La protein is one of the telomerase components interacting with hTR [14]; however, the functional relevance of La protein for telomerase activity has not yet been validated.

The FLAG-tagged La protein expression vector pCMV-La-FLAG or short-hairpin RNA for La protein expression vector pSh-La was transfected into Huh-7 cells, and transduction was confirmed by Western blotting using anti-FLAG antibody or anti-La protein antibody (Figure 5*A*). Telomerase activity detected by the TRAP assay in cells overexpressing La protein was significantly higher than that found in control cells. In contrast, telomerase activity was repressed in La protein–repressed Huh-7 cells (Figure 5*B*). To reveal the mechanism underlying the up-regulation of telomerase activity by La protein, we measured the changes in the expression of human telomerase reverse transcriptase and hTR by RTD-PCR. Although no significant changes were observed in the expression of human telomerase

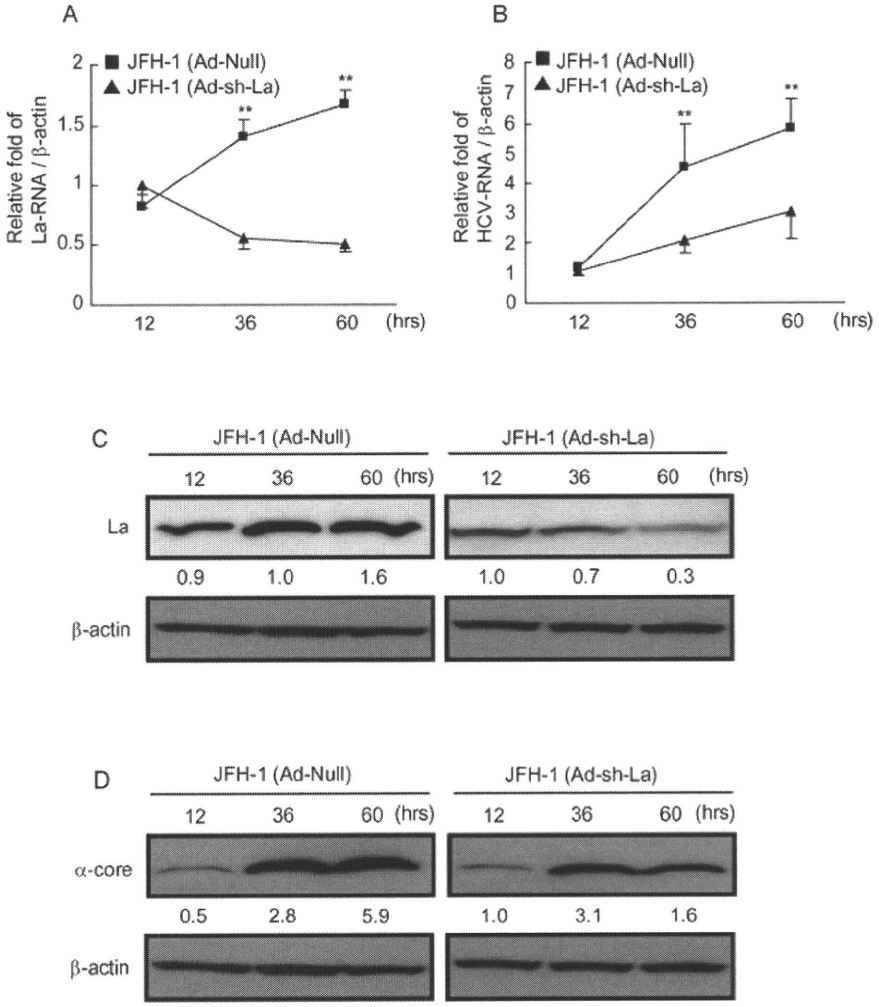

Figure 7. Suppression of La protein expression and its effect on of hepatitis C Virus (HCV) replication. *A*, Effect of Ad-shLa on La protein expression in JFH-1-transfected cells. $^{**}P < .01$. *B*, Effect of Ad-shLa on HCV replication. $^{**}P < .01$. *C*, Western blotting of La protein in JFH-1-transfected Huh-7.5 cells after infection with Ad-Null or Ad-shLa. *D*, Western blotting of HCV core protein in JFH-1-transfected Huh-7.5 cells after infection with Ad-Null or Ad-shLa.

reverse transcriptase, the expression of hTR was modestly but significantly increased by the overexpression of La protein and decreased by the repression of La protein, respectively (Figure 5*C*).

This finding was confirmed in Huh-7.5 cells transfected with JFH-1 RNA, which showed significantly higher expression of hTR than those transfected with translation-replication incompetent JFH-1 338U (Figure 5*D*). Moreover, JFH-1 infection similarly activated telomerase activity (Figure 5*E*) and induced hTR (Figure 5*F*) in Huh-7.5 cells, whereas JFH-1 338U infection did not activate telomerase activity or induce hTR. Therefore, the data strongly suggest that HCV infection could activate telomerase activity by increasing La protein and hTR.

When the relationship between La protein and telomerase components was evaluated in tissue biopsy specimens from patients with chronic hepatitis C, the expression of La protein strongly correlated with hTR. Moreover, it correlated significantly with the representative telomerase components p23 and HSP90 (Figure 6).

Repression of replication of JFH-1 in Huh-7.5 cells by recombinant adenovirus expressing short-hairpin RNA against La protein. Expression of La protein is induced by HCV infection, and it activates telomerase activity in Huh-7.5 cells. Therefore, it could be important to suppress La protein not only for the inhibition of HCV, but also for reducing the oncogenic potential of hepatocytes infected with HCV.

We constructed recombinant adenovirus expressing short-hairpin RNA against La protein (Ad-shLa). JFH-1 RNA was transfected into Huh-7.5 cells and 12 h after transfection, cells were exposed with Ad-shLa or control adenovirus (Ad-Null) for 1 h. At 12, 36, and 60 h after injection, changes in the levels of HCV RNA and La protein were evaluated by RTD-PCR and

Western blotting (Figure 7). At 60 h after injection, Ad-shLa repressed the level of La protein to 30% of that in the control cells (Figure 7*A*, 7*C*). Under these conditions, JFH-1 replication was significantly repressed to 50% at the RNA level (Figure 7*B*) and to 30% at the protein level (Figure 7*D*) of the control.

DISCUSSION

The translation machinery of HCV is simple and requires only the ribosomal 40s subunit, eIF2/GTP/Met-tRNA complex, and eIF3 to initiate translation [15]. However, many other canonical and noncanonical translation initiation factors interact with the HCV IRES and might regulate HCV translation [15]. However, the functional relevance of these factors for HCV replication has not yet been fully clarified.

Among 14 canonical and noncanonical translation initiation factors, we confirmed that La protein, PTB, eIF2γ, and PSMA7 had functional relevance for HCV IRES activity in RCF-26 cells. In the rabbit reticulocyte lysate, La protein, PTB, eIF3 p170, PCBP1, and PCBP2 significantly increased HCV IRES activity.

To evaluate the role of IRES activity in HCV replication, we constructed a translation incompetent infectious HCV clone, JFH-1 338U, by introducing a single-nucleotide mutation from A to U at nucleotide 338 in the 5′ nontranslated RNA that stabilized the stem-loop domain IV structure and impaired HCV translation, as reported elsewhere [12]. The La protein binds stem-loop IV, relaxes the stem-loop structure, and enhances HCV IRES activity [5].

Transfection of JFH-1 338U RNA into Huh-7.5 cells resulted in the production of neither HCV RNA nor HCV core protein. La protein overexpression could not overcome the replication defect by the 338U mutation (data not shown). These results indicate that JFH-1 338U was not only translation incompetent but also replication incompetent.

Interestingly, when the relationship between these initiation factors and HCV replication was investigated, we found that the initiation factors were induced by JFH-1 replication in Huh-7.5 cells. The relationship between these initiation factors and HCV replication was also evaluated in liver biopsy specimens from patients with chronic hepatitis C.

La protein has been reported to be one of the components of telomerase [14]; therefore, we evaluated the functional role of La protein on telomerase activity. Overexpression of La protein in Huh-7 cells increased telomerase activity significantly, as evaluated by the TRAP assay. The expression of hTR, an RNA template of human telomerase reverse transcriptase was increased. La protein could bind to the double-stranded RNA structure and possibly stabilize hTR. Importantly, JFH-1 infection activated telomerase activity and induced hTR in Huh-7.5 cells.

Interestingly, La protein significantly correlated with hTR, p23, and HSP90, representative telomerase components, in the tissue specimens from patients with chronic hepatitis C. Several reports have also shown a low but significant level of expression of human telomerase reverse transcriptase in regenerating hepatocytes in cirrhotic livers [16]. These hepatocytes could overcome cellular senescence and transform into tumor cells if the associated genetic or epigenetic changes occurred during the course of chronic hepatitis C infection.

In this study, we constructed recombinant adenovirus expressing short-hairpin RNA against La protein and successfully suppressed the replication of the infectious HCV clone JFH-1 for the first time, to our knowledge. The virological significance of La protein for HCV replication using infectious HCV clone has not been reported before to our knowledge [17].

Because La protein is essentially involved in HCV IRES activity, its production is induced by HCV itself, and it potentially activates telomerase activity, it might be an exceptionally good candidate therapeutic target. Additional research into the development of small molecules, such as small peptides and chemical compounds, that are active against La protein could be useful for the development of novel anti-HCV therapeutic agents.

Acknowledgments

We thank Mikiko Nakamura and Nami Nishiyama for excellent technical assistance. We also thank Professor C. M. Rice, of Rockefeller University, for kindly providing the Huh-7.5 cells.

References

1. Kiyosawa K, Sodeyama T, Tanaka E, et al. Interrelationship of blood transfusion, non-A, non-B hepatitis and hepatocellular carcinoma: analysis by detection of antibody to hepatitis C virus. Hepatology **1990**; 12: 671–675.
2. Fried MW, Shiffman ML, Reddy KR, et al. Peginterferon alfa-2a plus ribavirin for chronic hepatitis C virus infection. N Engl J Med **2002**; 347:975–982.
3. Hara H, Aizaki H, Matsuda M, et al. Involvement of creatine kinase B in hepatitis C virus genome replication through interaction with the viral NS4A protein. J Virol **2009**; 83:5137–5147.
4. Tsukiyama-Kohara K, Iizuka N, Kohara M, Nomoto A. Internal ribosome entry site within hepatitis C virus RNA. J Virol **1992**; 66: 1476–1483.
5. Ali N, Siddiqui A. The La antigen binds 5′ noncoding region of the hepatitis C virus RNA in the context of the initiator AUG codon and stimulates internal ribosome entry site-mediated translation. Proc Natl Acad Sci U S A **1997**; 94:2249–2254.
6. Ali N, Siddiqui A. Interaction of polypyrimidine tract-binding protein with the 5′ noncoding region of the hepatitis C virus RNA genome and its functional requirement in internal initiation of translation. J Virol **1995**; 69:6367–6375.
7. Honda M, Kaneko S, Matsushita E, Kobayashi K, Abell GA, Lemon SM. Cell cycle regulation of hepatitis C virus internal ribosomal entry site-directed translation. Gastroenterology **2000**; 118:152–162.
8. Honda M, Shimazaki T, Kaneko S. La protein is a potent regulator of replication of hepatitis C virus in patients with chronic hepatitis C through internal ribosomal entry site-directed translation. Gastroenterology **2005**; 128:449–462.
9. Shimazaki T, Honda M, Kaneko S, Kobayashi K. Inhibition of internal

ribosomal entry site-directed translation of HCV by recombinant IFN-α correlates with a reduced La protein. Hepatology **2002**; 35:199–208.
10. Honda M, Kaneko S, Kawai H, Shirota Y, Kobayashi K. Differential gene expression between chronic hepatitis B and C hepatic lesion. Gastroenterology **2001**; 120:955–966.
11. Wakita T, Pietschmann T, Kato T, et al. Production of infectious hepatitis C virus in tissue culture from a cloned viral genome. Nat Med **2005**; 11:791–796.
12. Honda M, Brown EA, Lemon SM. Stability of a stem-loop involving the initiator AUG controls the efficiency of internal initiation of translation on hepatitis C virus RNA. RNA **1996**; 2:955–968.
13. Forsythe HL, Jarvis JL, Turner JW, Elmore LW, Holt SE. Stable association of hsp90 and p23, but not hsp70, with active human telomerase. J Biol Chem **2001**; 276:15571–15574.
14. Ford LP, Shay JW, Wright WE. The La antigen associates with the human telomerase ribonucleoprotein and influences telomere length in vivo. RNA **2001**; 7:1068–1075.
15. Pestova TV, Shatsky IN, Fletcher SP, Jackson RJ, Hellen CU. A prokaryotic-like mode of cytoplasmic eukaryotic ribosome binding to the initiation codon during internal translation initiation of hepatitis C and classical swine fever virus RNAs. Genes Dev **1998**; 12:67–83.
16. Kawakami Y, Kitamoto M, Nakanishi T, et al. Immuno-histochemical detection of human telomerase reverse transcriptase in human liver tissues. Oncogene **2000**; 19:3888–3893.
17. Xue Q, Ding H, Liu M, et al. Inhibition of hepatitis C virus replication and expression by small interfering RNA targeting host cellular genes. Arch Virol **2007**; 152:955–962.

Cancer Research

Oncostatin M Renders Epithelial Cell Adhesion Molecule–Positive Liver Cancer Stem Cells Sensitive to 5-Fluorouracil by Inducing Hepatocytic Differentiation

Taro Yamashita, Masao Honda, Kouki Nio, Yasunari Nakamoto, Tatsuya Yamashita, Hiroyuki Takamura, Takashi Tani, Yoh Zen, and Shuichi Kaneko

Abstract

Recent evidence suggests that a certain type of hepatocellular carcinoma (HCC) is hierarchically organized by a subset of cells with stem cell features (cancer stem cells; CSC). Although normal stem cells and CSCs are considered to share similar self-renewal programs, it remains unclear whether differentiation programs are also maintained in CSCs and effectively used for tumor eradication. In this study, we investigated the effect of oncostatin M (OSM), an interleukin 6–related cytokine known to induce the differentiation of hepatoblasts into hepatocytes, on liver CSCs. OSM receptor expression was detected in the majority of epithelial cell adhesion molecule–positive ($EpCAM^+$) HCC with stem/progenitor cell features. OSM treatment resulted in the induction of hepatocytic differentiation of $EpCAM^+$ HCC cells by inducing signal transducer and activator of transcription 3 activation, as determined by a decrease in stemness-related gene expression, a decrease in EpCAM, α-fetoprotein and cytokeratin 19 protein expressions, and an increase in albumin protein expression. OSM-treated $EpCAM^+$ HCC cells showed enhanced cell proliferation with expansion of the EpCAM-negative non-CSC population. Noticeably, combination of OSM treatment with the chemotherapeutic agent 5-fluorouracil (5-FU), which eradicates EpCAM-negative non-CSCs, dramatically increased the number of apoptotic cells *in vitro* and suppressed tumor growth *in vivo* compared with either saline control, OSM, or 5-FU treatment alone. Taken together, our data suggest that OSM could be effectively used for the differentiation and active cell division of dormant $EpCAM^+$ liver CSCs, and the combination of OSM and conventional chemotherapy with 5-FU efficiently eliminates HCC by targeting both CSCs and non-CSCs. *Cancer Res; 70(11); 4687–97. ©2010 AACR.*

Introduction

It is widely accepted that cancer is a disease that develops from a normal cell with accumulated genetic/epigenetic changes. Although considered monoclonal in origin, cancer is composed of heterogeneous cellular populations. These heterogeneities are traditionally explained by the clonal evolution of cancer cells through a series of stochastic genetic events (clonal evolution model; ref. 1). In contrast, cancer cells are known to have the capabilities characteristic of stem cells with respect to self-renewal, limitless division, and generation of heterogeneous cell populations. Recent evidence suggests that tumor cells possess stem cell features (cancer stem cells; CSC) to self-renew and give rise to relatively differentiated cells through asymmetric division, and thereby form heterogeneous populations (CSC model; refs. 2, 3). Accumulating evidence supports the notion that CSCs could generate tumors more efficiently in immunodeficient mice than non-CSCs in the case of leukemia and various solid tumors (4–9), although the origin of CSCs is still a controversial issue.

Worldwide, hepatocellular carcinoma (HCC) is one of the most common malignancies with poor outcome (10). Recent evidence suggests that at least some HCCs are organized by liver CSCs in a hierarchical manner (11). Several markers have been identified as useful for the enrichment of liver CSCs, including side population fraction (12), CD133 (13), CD90 (14), and OV6 (15). We have recently used epithelial cell adhesion molecule (EpCAM) and α-fetoprotein (AFP) to identify novel prognostic HCC subtypes related to certain developmental stages of human liver lineages (16). Among these, EpCAM-positive ($^+$) AFP^+ HCC (hepatic stem cell–like HCC) is characterized by young onset of disease, activation of Wnt/β-catenin signaling, and poor prognosis. *EPCAM* is a target gene of Wnt/β-catenin signaling (17), and we previously identified that $EpCAM^+$ HCC cells from primary HCC

Authors' Affiliation: Center for Liver Diseases, Kanazawa University Hospital, Kanazawa, Ishikawa, Japan

Note: Supplementary data for this article are available at Cancer Research Online (http://cancerres.aacrjournals.org/).

Corresponding Authors: Taro Yamashita, Department of Gastroenterology, Kanazawa University Graduate School of Medical Science, 13-1 Takara-Machi, Kanazawa, Ishikawa 920-8641, Japan. Phone: 81-76-265-2851; Fax: 81-76-265-4250; E-mail: taroy@m-kanazawa.jp and Shuichi Kaneko, Center for Liver Diseases, Kanazawa University Hospital; Department of Gastroenterology, Kanazawa University Graduate School of Medical Science, 13-1 Takara-Machi, Kanazawa, Ishikawa 920-8641, Japan. Phone: 81-76-265-2230; Fax: 81-76-265-4250; E-mail: skaneko@m-kanazawa.jp.

doi: 10.1158/0008-5472.CAN-09-4210

samples and cell lines have the features of CSCs, at least in the hepatic stem cell–like HCC subtype (18). Thus, EpCAM seems to be a potentially useful marker for the isolation of liver CSCs in hepatic stem cell–like HCC.

CSCs are considered to be resistant to chemotherapy and radiotherapy (19–21), which may be associated with the recurrence of the tumor after treatment. These findings have led to the proposal of "destemming" CSCs, to induce the differentiation of CSCs into non-CSCs or to eradicate CSCs by inhibiting the signaling pathway responsible for self-renewal (22). Recent studies support this proposal and suggest the utility of bone morphogenetic proteins, activated during embryogenesis and required for differentiation of neuronal stem cells, to induce differentiation of brain CSCs and facilitate brain tumor eradication (23, 24). However, it is still debatable whether simple differentiation of CSCs effectively eradicates tumors (25).

Oncostatin M (OSM), an interleukin (IL)-6–related cytokine produced by $CD45^+$ hematopoietic cells, is known to enhance hepatocytic differentiation of hepatoblasts by inducing the activation of the signal transducer and activator of transcription 3 (STAT3) pathway (26). Although OSM, IL-6, and leukemia-inhibitory factor share STAT3 signaling cascades, OSM is known to exploit the distinct hepatocytic differentiation signaling in an OSM receptor (OSMR)–specific manner (27). In this study, we hypothesized that OSM induces hepatocytic differentiation of liver CSCs through the OSMR signaling pathway. We examined OSMR expression and the effect of OSM in $EpCAM^+$ HCC in terms of hepatocytic differentiation and antitumor activities.

Materials and Methods

Clinical HCC specimens

A total of 107 HCC tissues and adjacent noncancerous liver tissues were obtained from patients who underwent hepatectomy for HCC treatment from 1999 to 2007 in Kanazawa University Hospital. These samples were formalin-fixed and paraffin-embedded, and used for immunohistochemistry. HCC and adjacent noncancerous liver tissues were histologically diagnosed by two pathologists. An additional fresh $EpCAM^+$ AFP^+ HCC sample was obtained from a surgically resected specimen and immediately used for the preparation of single-cell suspensions and xenotransplantation. All tissue acquisition procedures were approved by the Ethics Committee and the Institutional Review Board of Kanazawa University Hospital. All patients provided written informed consent.

Cell culture and reagents

HuH1 and HuH7 cells were cultured as previously described (18). A primary HCC tissue was dissected and digested in 1 μg/mL of type 4 collagenase (Sigma-Aldrich Japan K.K.) solution at 37°C for 15 to 30 minutes. Contaminated RBC were lysed with ammonium chloride solution (STEMCELL Technologies) on ice for 5 minutes. $CD45^+$ leukocytes and Annexin V^+ apoptotic cells were removed by autoMACS-pro cell separator and magnet beads (Miltenyi Biotec K.K.). EpCAM-positive and -negative cells were enriched by autoMACS-pro cell separator and CD326 (EpCAM) MicroBeads (Miltenyi Biotec K.K.). Recombinant OSM was purchased from R&D Systems, Inc. 5-Fluorouracil (5-FU) was obtained from Kyowa Kirin.

Quantitative reverse transcription-PCR analysis

Total RNA was extracted using TRIzol (Invitrogen) according to the instructions of the manufacturer. The expression of selected genes was determined in triplicate using the 7900 Sequence Detection System (Applied Biosystems). Each sample was normalized relative to β-actin expression. Probes used were *TACSTD1*, Hs00158980_m1; *AFP*, Hs00173490_m1; *KRT19*, Hs00761767_s1; *hTERT*, Hs00162669_m1; *Bmi1*, Hs00180411_m1; *POU5F1*, Hs00999632_g1; *CYP3A4*, Hs00430021_m1; *OSMR*, Hs00384278_m1; and *ACTB*, Hs99999903_m1 (Applied Biosystems).

Western blotting

Whole cell lysates were prepared using radioimmunoprecipitation assay lysis buffer as described previously (28). Rabbit polyclonal antibodies to STAT3 (Cell Signaling Technology, Inc.), rabbit polyclonal anti-OSMR antibodies H-200 (Santa Cruz Biotechnology), mouse monoclonal anti–phosphorylated STAT3 (Tyr^{705}) antibody (3E2; Cell Signaling Technology), and mouse monoclonal anti–β-actin antibody (Sigma-Aldrich) were used. Immune complexes were visualized by enhanced chemiluminescence (Amersham Biosciences, Corp.) as described by the manufacturer.

Immunohistochemistry and immunofluorescence analyses

Immunohistochemistry was performed using Envision+ kits (DAKO) according to the instructions of the manufacturer. Anti-EpCAM monoclonal antibody, VU-1D9 (Oncogene Research Products), was used for detecting EpCAM. Goat anti-OSMR polyclonal antibodies (C-20) were obtained from Santa Cruz Biotechnology. Mouse anti-CYP3A4 polyclonal antibodies (Abnova), mouse anti–cytokeratin (CK) 19 monoclonal antibody (DAKO), and mouse anti–Ki-67 monoclonal antibody MIB-1 (DAKO) were used for detecting CYP3A4, CK19, and Ki-67, respectively. Samples with >5% positive staining in a given area for a particular antibody were considered to be positive. For immunofluorescence analyses, anti-EpCAM antibody (Oncogene Research Products), anti-gp130ST antibodies (Santa Cruz Biotechnology), and anti–phosphorylated STAT3 (Tyr^{705}) antibody (3E2; Cell Signaling Technology) were used. Alexa 488 FITC-conjugated anti-mouse IgG or Alexa 568 Texas red–conjugated anti-goat/rabbit IgG (Molecular Probes) were used as secondary antibodies. Confocal fluorescence microscopic analysis was performed essentially as previously described (18).

Fluorescence-activated cell sorting analyses

Cultured cells were trypsinized, washed, and resuspended in HBSS (Lonza) supplemented with 1% HEPES and 2% fetal bovine serum (FBS). Cells were then incubated with FITC-conjugated anti-EpCAM monoclonal antibody Clone Ber-EP4 (DAKO) on ice for 30 minutes, and analyzed using

a FACSCalibur (BD Biosciences). Intracellular AFP, CK19, and albumin levels were examined using a BD Cytofix/Cytoperm Fixation/Permeabilization Kit (BD Biosciences), anti-AFP mouse monoclonal antibody (Nichirei Biosciences Inc.), anti-CK19 mouse monoclonal antibody (DAKO), and rabbit polyclonal anti-albumin antibodies (Cell Signaling Technology), respectively.

Cell proliferation and colony formation assay

For cell proliferation assays, 2×10^3 cells were seeded in 96-well plates and cultured with 1% FBS DMEM (control), 1% DMEM with OSM (100 ng/mL), 5-FU (2 μg/mL), or OSM (100 ng/mL) and 5-FU (2 μg/mL) for 3 to 7 days without media changes. Cell viability was evaluated in quadruplicate using a CellTiter 96 AQueous kit (Promega). For colony formation assays, 1×10^3 cells were harvested in a one-well Culture Slide (BD Biosciences) and cultured with 1% FBS DMEM (control) with or without OSM (100 ng/mL). Culture medium was replaced every 3 days and the colonies were fixed with ice-cold 100% methanol and used for immunofluorescence 10 days after the initiation of treatment.

RNA interference

SiRNAs specific to OSMR (Silencer Select siRNA S17542) and a control siRNA (Silencer Select Negative Control no. 1) were obtained from Ambion (Applied Biosystems). To each well of a six-well plate, 2×10^5 cells were seeded 12 hours before transfection. Transfection was performed using LipofectAMINE 2000 (Invitrogen), according to the instructions of the manufacturer. A total of 100 pmol/L of siRNA duplex was used for each transfection.

Apoptosis assay

Cells were cultured in 1% FBS DMEM (control), 1% FBS DMEM with OSM (100 ng/mL), 5-FU (2 μg/mL), or OSM (100 ng/mL) and 5-FU (2 μg/mL) for 3 days in six-well plates or in culture slides (BD Biosciences). Annexin V binding to cell membranes was visualized using Annexin V-FITC antibodies and a FACSCalibur flow cytometer (BD Biosciences). Activation of caspase 3 was visualized by immunohistochemistry or immunofluorescence using anti-active caspase-3 polyclonal antibodies (Promega), as described by the manufacturer.

Animal studies

Six-week-old NOD/SCID mice (NOD/NCrCRl-*Prkdc*^{scid}) were purchased from Charles River Laboratories, Inc. The protocol was approved by the Kanazawa University Animal Care and Use Committee. One million tumor cells were suspended in 200 μL of DMEM and Matrigel (1:1), and a s.c. injection was performed. The incidence and size of subcutaneous tumors were recorded. Intratumoral injections of 50 μL of PBS (control), OSM (2 μg/tumor), 5-FU (250 μg/tumor), or OSM (2 μg/tumor) and 5-FU (250 μg/tumor) were initiated twice weekly 48 days after the injection of tumor cells when the average volume of four tumors in each group had reached 400 mm^3. For histologic evaluation, tumors were formalin-fixed and paraffin-embedded.

Statistical analyses

The association of OSMR expression and clinicopathologic characteristics in HCC was examined using either Mann-Whitney U or χ^2 tests. Student's t test was used to compare various test groups assayed by quantitative reverse transcription-PCR analysis. All analyses were performed using GraphPad Prism software.

Results

Distinct expression of OSMRs in HCC

Before exploring the effect of OSM on HCC, we examined the expression of its receptor, OSMR, in surgically resected HCC and adjacent noncancerous liver tissues by immunohistochemistry. Representative staining of OSMRs in tumor/nontumor tissues is shown in Fig. 1A. In general, cell surface and cytoplasmic immunoreactivity to OSMR were rarely detected in hepatocytes in chronic hepatitis liver (a), but were frequently detected in small hepatocyte-like cells in the stroma or transitional cells in the lobule of cirrhotic liver (b), as indicated by the arrows. Note that immunoreactivity to OSMR was not detected in bile duct epithelia or ductular reactions in which EpCAM$^+$ hepatic progenitor cells are thought to accumulate (Supplementary Fig. S1), suggesting that OSMRs might be expressed in hepatic progenitor cells committed to hepatocytes. Immunoreactivity to OSMRs was more strongly detected in HCC than in noncancerous liver (c), and the expression was heterogeneous in the tumor. Of note, OSMRs were detected in HCC cells at the invasive front area of the tumor (d) where CSCs are known to invade frequently (arrows).

Immunoreactivity to OSMR antibodies and EpCAM antibodies was detected in 66 (61.7%) and 38 (35.5%) of 107 HCC specimens, respectively. The clinicopathologic characteristics of OSMR$^+$ and OSMR$^-$ HCC cases are shown in Table 1. OSMR$^+$ HCC was characterized by high serum AFP values ($P = 0.009$), poorly differentiated morphology ($P < 0.0001$), and a high frequency of EpCAM$^+$ HCCs ($P = 0.024$), suggesting that the OSMR is expressed in HCC with stem/progenitor cell features. OSMR$^+$ HCC was also characterized by young onset of disease and male dominance, although these features did not reach statistical significance ($P = 0.052$ and 0.058, respectively). OSMR was more frequently detected in EpCAM$^+$ HCCs (76.3%) than in EpCAM$^-$ HCCs (53.7%). Expression of OSMR and EpCAM was further investigated by double immunofluorescence analysis, and immunoreactivity to OSMR was detected in both EpCAM$^+$ normal hepatic progenitors (Fig. 1B) and EpCAM$^+$ HCC cells (Fig. 1C). These data suggest that although OSMR is more widely expressed than EpCAM in HCC, OSMR is frequently expressed in EpCAM$^+$ normal hepatic progenitors and liver CSCs.

OSM induces hepatocytic differentiation of EpCAM+ HCC

Because OSMR was expressed in the majority of EpCAM$^+$ HCCs, we investigated the effect of OSM on EpCAM$^+$ HCC cell lines. First, we examined the expression of OSMR and its signal transducer glycoprotein 130 (gp130) in EpCAM$^+$ AFP$^+$ HCC cell lines HuH1 and HuH7 by immunofluorescence

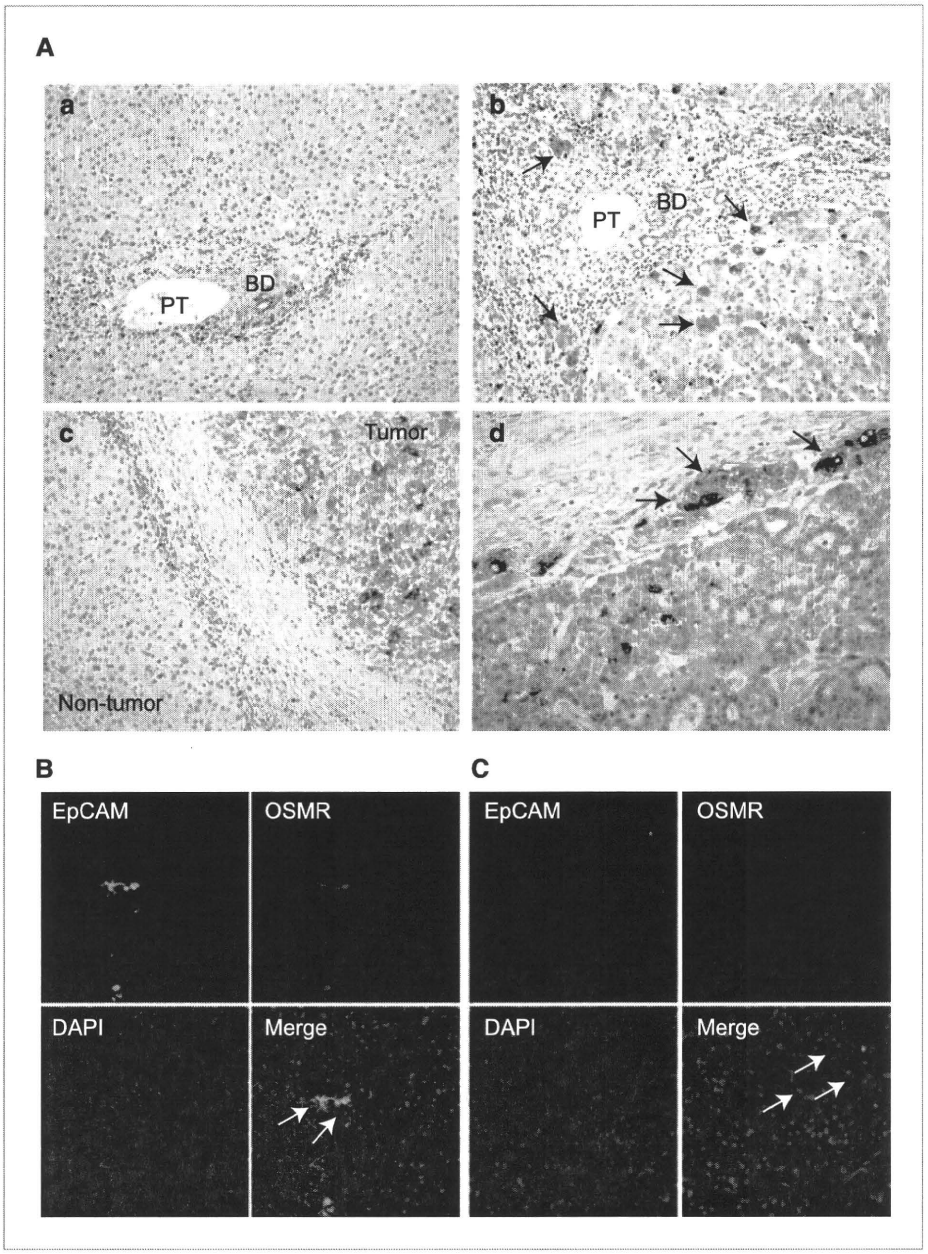

Figure 1. A, representative images of OSMR staining in noncancerous liver tissues and HCC tissues. Immunoreactivity to OSMR was not detected in hepatocytes in chronic hepatitis liver tissue (a) but was detected in a subset of small hepatocyte-like cells in the stroma or transitional cells in the lobule (b, arrows) of cirrhotic liver tissue. OSMR was more abundantly expressed in HCC than in noncancerous liver (c). $OSMR^+$ cancer cells were disseminated in the invasive front area of the tumor (d, arrows). PT, portal tract; BD, bile duct. B and C, double immunofluorescence analysis of EpCAM (green) and OSMR (red) expression in noncancerous (B) and HCC (C) tissues.

(Fig. 2A). Both gp130 and OSMR protein expressions were detected in these cells, consistent with the immunohistochemical data. Because OSM is known to induce the hepatocytic differentiation of hepatoblasts in a STAT3-dependent manner, we investigated the effect of OSM on phosphorylation of STAT3 in HuH1 and HuH7 cells by immunofluorescence and Western blotting. Incubation of HCC cells for 1 hour with OSM at a concentration of 100 ng/mL resulted in the induction and nuclear accumulation of phosphorylated STAT3 compared with controls (Fig. 2B and C). We examined the effect of OSM on the $EpCAM^+$ cell population in HuH1 and HuH7 cells. We first labeled HuH1 and HuH7 cells with CD326 (EpCAM) MicroBeads and FITC-conjugated anti-EpCAM antibodies (Clone Ber-EP4) and performed positive/negative selection using magnetic activated cell sorting to determine the appropriate gating criteria for EpCAM-high (designated as $EpCAM^+$) and EpCAM-low/negative (designated as $EpCAM^-$) cell population (Fig. 2D, top). It is interesting that OSM treatment (100 ng/mL for 72 hours) diminished the $EpCAM^+$ cell population from 50.7% to 10.1% in HuH1 and from 55.2% to 28.8% in HuH7 cells when the same constant gating criteria was applied (Fig. 2D, bottom).

We used RNA interference to investigate whether the decrease in $EpCAM^+$ cells by OSM treatment depends on the expression of OSMR. Transfection of siRNAs specific to *OSMR* (si-OSMR) resulted in the knockdown of target genes

compared with the control (si-Control) in HuH1 and HuH7 cells 48 hours after transfection (Supplementary Fig. S2A). We further confirmed the decrease of OSMR protein expression by immunofluorescence and Western blotting 72 hours after transfection (Supplementary Fig. S2B and C). When we treated these HuH1 and HuH7 cells with OSM (100 ng/mL) for 1 hour, we observed the decrease of phosphorylated STAT3 by *OSMR* gene silencing compared with the control (Supplementary Fig. S2C). Furthermore, OSM-mediated decrease in the number of EpCAM$^+$ cells was inhibited by *OSMR* gene silencing (Supplementary Fig. S2D), suggesting that OSM exploits the diminution of EpCAM$^+$ cells through the activation of the OSMR signaling pathway in EpCAM$^+$ HCC.

We further examined the effect of OSM on hepatocytic differentiation by quantitative reverse transcription-PCR and fluorescence-activated cell sorting (FACS) analyses. OSM treatment in HuH1 cells reduced the expression of hepatic progenitor–related genes including *AFP, KRT19* (encoding CK19), and *TERT* (encoding telomerase reverse transcriptase; TERT; Fig. 3A). OSM treatment further reduced the expression of *BMI1* and *POU5F1* (encoding Oct4), which is known to be expressed and required for self-renewal in embryonic stem cells. OSM treatment also increased the expression of the hepatocyte marker, *CYP3A4*. Furthermore, OSM treatment reduced AFP$^+$ and CK19$^+$ cells and increased albumin$^+$ cells compared with the untreated controls, as evaluated by the geometric mean of the fluorescence intensities of whole cells analyzed by intracellular FACS (Fig. 3B). Similar results were obtained in HuH7 cells (data not shown) and, taken together, these data suggest that OSM induced the hepatocytic differentiation of EpCAM$^+$ HCCs.

Hepatocytic differentiation of EpCAM+ HCC by OSM augments cell proliferation

In general, normal stem cells are more quiescent than differentiated cells in terms of cell division. We therefore evaluated the effect of OSM on cell proliferation in HuH1 and HuH7 cells. It is interesting that OSM treatment for 10 days resulted in a larger colony formation following treatment with OSM (100 ng/mL) compared with untreated controls. Of note, the majority of cells comprising these larger colonies were EpCAM$^-$, or had low expression levels, whereas a subset of untreated control cells maintained high EpCAM expression (Fig. 3C). Similar results were obtained when cell proliferation was examined using a [3-(4, 5-dimethylthiazol-2-yl)-5-(3-carboxymethoxyphenyl)-2-(4-sulfophenyl)-2H-tetrazolium] tetrazolium assay and Ki-67 labeling index (Fig. 3D). OSM modestly enhanced cell proliferation (top) and increased Ki-67–positive cells (middle and bottom) compared with untreated controls in both HuH1 and HuH7 cells with statistical significance (Fig. 3D).

OSM treatment increases chemosensitivity of EpCAM+ HCC

The abovementioned data imply that although OSM may induce the hepatocytic differentiation of dormant EpCAM$^+$ liver CSCs, OSM treatment alone might instead enhance cell proliferation through expansion of amplifying differentiated cancer cells *in vitro*, raising the question of efficacy of differentiation therapy in EpCAM$^+$ HCC. Because rapidly amplifying cells are considered to be more sensitive to chemotherapeutic agents, we investigated the effect of combining OSM treatment with conventional chemotherapy to target both dormant CSCs and amplifying non-CSCs. We have shown that 5-FU treatment

Table 1. Clinicopathologic characteristics of OSMR$^+$ and OSMR$^-$ HCC cases used for immunohistochemical analyses

Variables	OSMR$^+$ (n = 66)	OSMR$^-$ (n = 41)	P*
Age (years, mean ± SE)	62.7 ± 1.3	66.4 ± 1.3	0.052
Sex (male/female)	55/11	27/14	0.058
Etiology (HBV/HCV/other)	25/35/6	8/30/3	0.10
Liver cirrhosis (yes/no)	43/23	26/15	1.0
AFP (ng/mL, mean ± SE)	6,453 ± 5901	1,039 ± 935	0.009
Histologic grade†			
I–II	3	16	
II–III	54	20	
III–IV	9	5	<0.0001
Tumor size (<3 cm/>3 cm)	30/36	15/26	0.42
Tumor-node-metastasis classification			
I/II	48	31	
III/IV	18	10	0.82
EpCAM (positive/negative)	29/37	9/32	0.024

*Mann-Whitney U test or χ^2 test.
†Edmondson-Steiner.

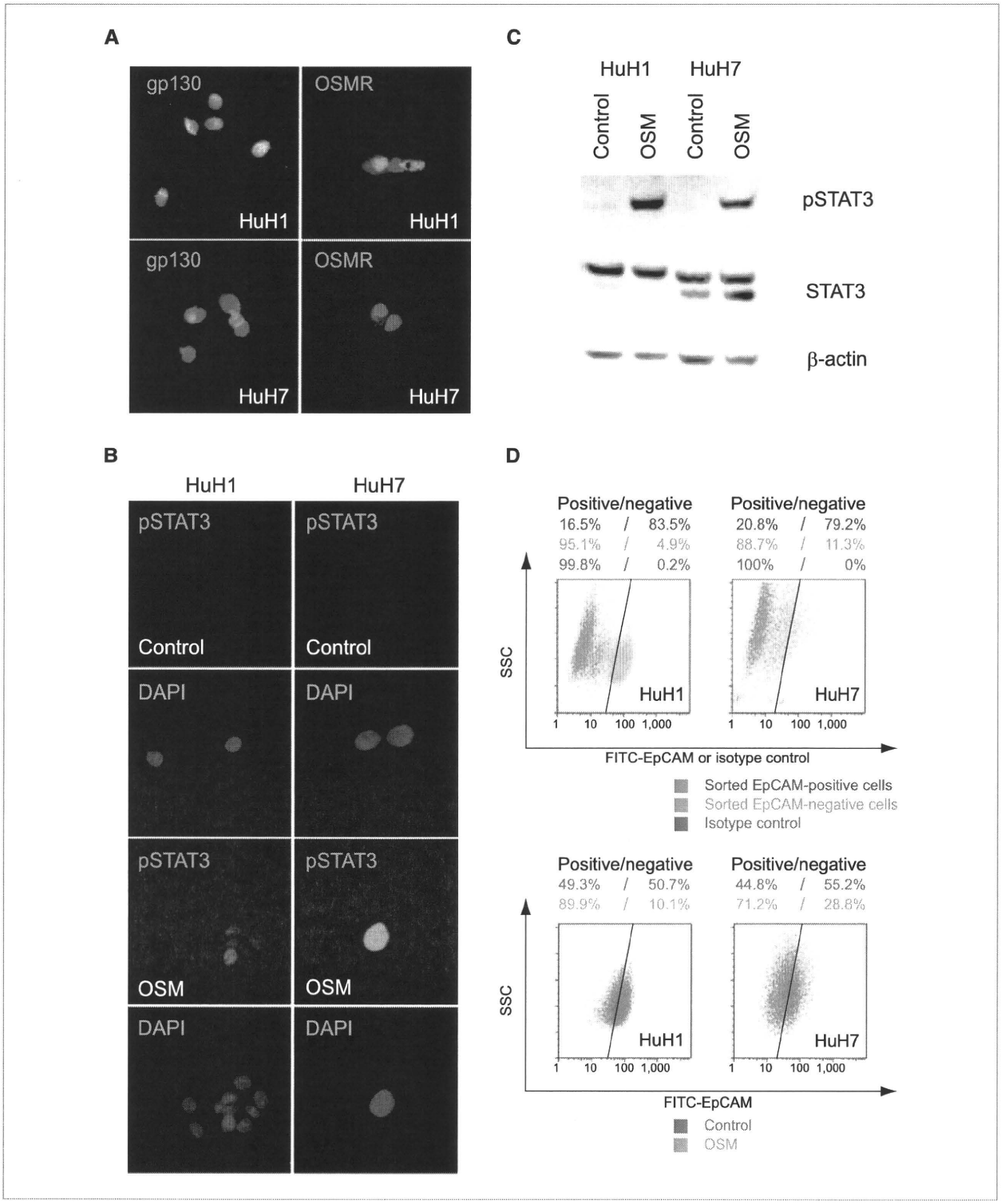

Figure 2. A, immunofluorescence analysis of gp130 and OSMR expression in HuH1 and HuH7 cell lines. B, immunofluorescence analysis of phosphorylated STAT3 expression in HuH1 and HuH7 cell lines stimulated by OSM (100 ng/mL for 1 hour) and controls. C, Western blotting analysis of whole or phosphorylated STAT3 protein expression in HuH1 and HuH7 cells stimulated by OSM (100 ng/mL for 1 hour) and controls. D, FACS analysis of HuH1 and HuH7 cells stained with FITC-conjugated anti-EpCAM antibodies. Top, EpCAM-high (designated as $EpCAM^+$; yellow) and EpCAM-low/negative cells (designated as $EpCAM^-$; blue) were enriched by magnetic activated cell sorting and labeled with FITC-conjugated anti-EpCAM antibodies or isotype control antibodies. Bottom, cells were cultured in 1% FBS DMEM with (green) or without OSM (100 ng/mL; orange) for 3 days and stained with FITC-conjugated anti-EpCAM antibodies.

alone could diminish EpCAM⁻ non-CSCs which results in the enrichment of EpCAM⁺ CSCs in HCC (18). We therefore explored the effect of 5-FU in combination with OSM on EpCAM⁺ HCC cell proliferation and apoptosis *in vitro*.

When HuH1 and HuH7 cells were treated with OSM alone and cultured for 7 days, cell proliferation was modestly increased compared with untreated controls (Fig. 4A). In contrast, 5-FU treatment clearly inhibited cell proliferation.

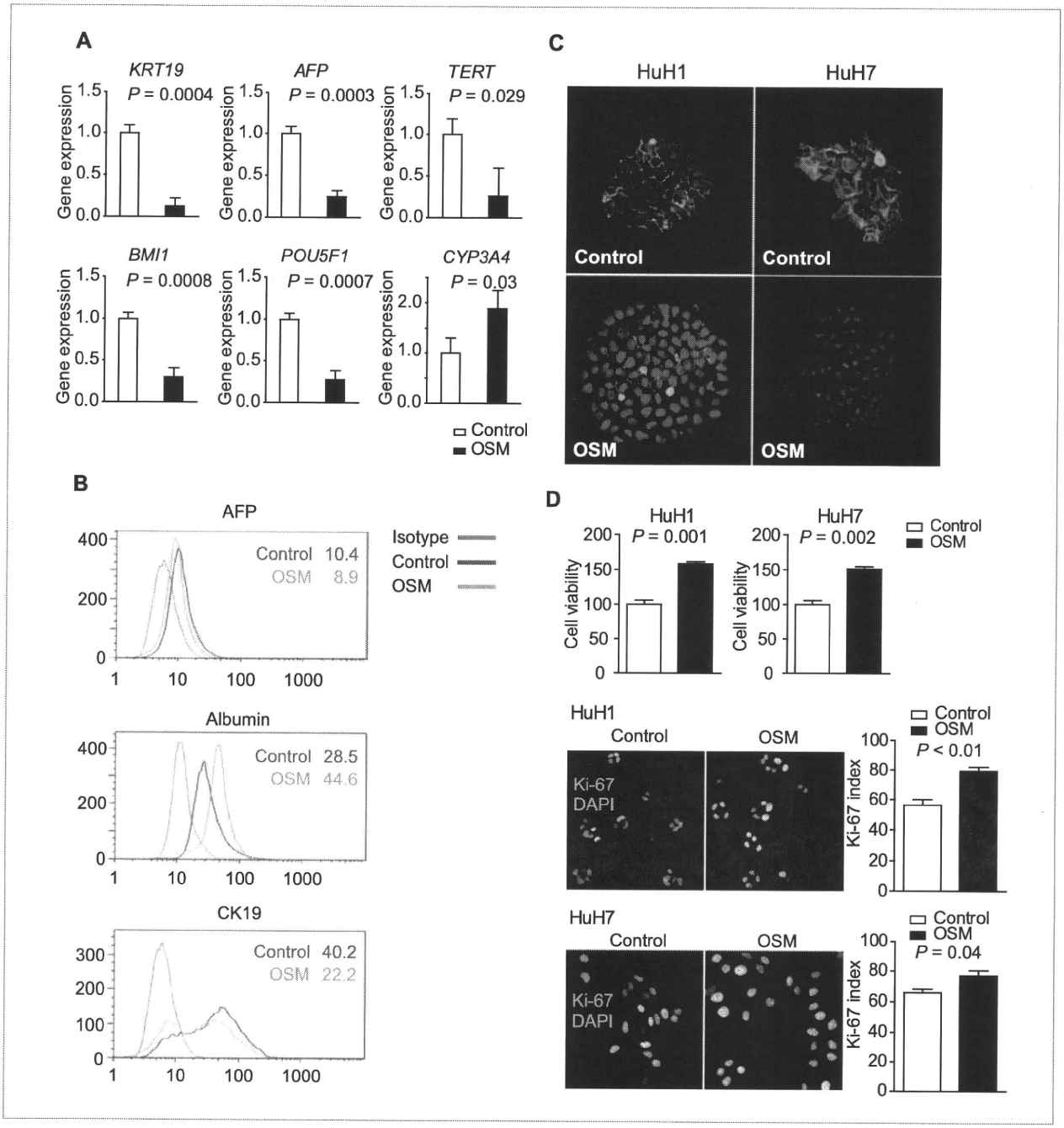

Figure 3. A, quantitative reverse transcription-PCR analysis of HuH1 cells cultured in 1% FBS DMEM with (black columns) or without (white columns) OSM (100 ng/mL) for 3 days. B, intracellular FACS analysis of HuH1 cells cultured in 1% FBS DMEM with (green line) or without (red line) OSM (100 ng/mL) for 3 days. The number in the figure indicates the geometric mean of the fluorescence intensity on a logarithmic scale. C, immunofluorescence analysis of HuH1 and HuH7 cell colonies cultured in 1% FBS DMEM with or without OSM (100 ng/mL) for 10 days. Colonies were fixed with 100% ice-cold methanol and stained with FITC-conjugated anti-EpCAM antibodies. D, top, cell proliferation assay of HuH1 and HuH7 cells cultured in 1% FBS DMEM with (black column) or without (white column) OSM (100 ng/mL) for 3 days. Middle and bottom, immunofluorescence analysis of HuH1 and HuH7 cells cultured in 1% FBS DMEM with or without OSM (100 ng/mL) for 3 days. Cells were fixed with 100% ice-cold methanol and stained with anti–Ki-67 antibodies.

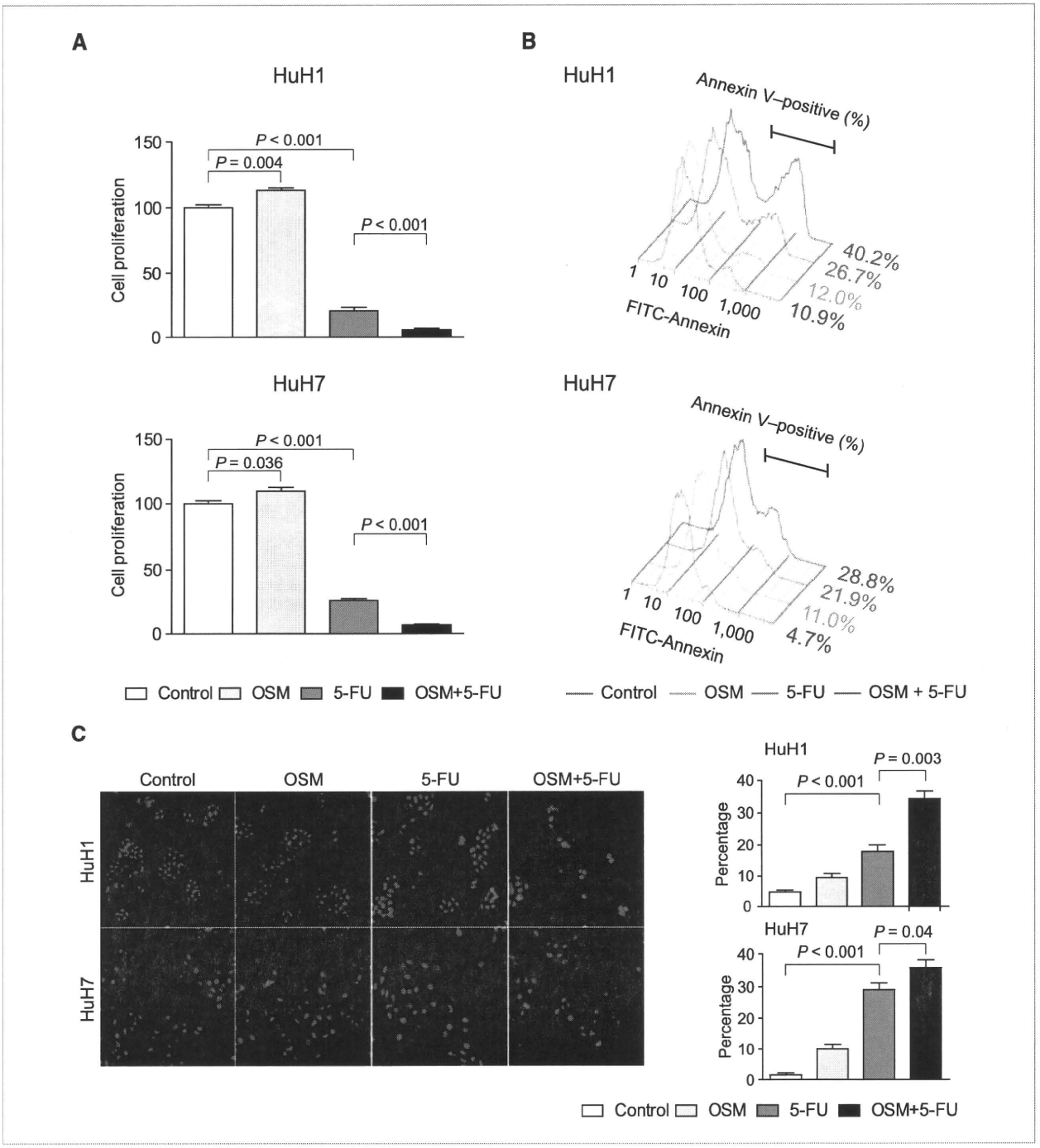

Figure 4. A, cell proliferation assay of HuH1 and HuH7 cells cultured in 1% FBS DMEM with OSM (100 ng/mL; light gray columns), 5-FU (2 μg/mL; gray columns), OSM (100 ng/mL) and 5-FU (2 μg/mL; black columns), or PBS as control (white columns) for 7 days. B, FACS analysis of HuH1 and HuH7 cells stained with FITC-conjugated anti–Annexin V antibodies. Cells were cultured in 1% FBS DMEM with OSM (100 ng/mL; green line), 5-FU (2 μg/mL; blue line), OSM (100 ng/mL) and 5-FU (2 μg/mL; red line), or PBS as control (gray line) for 3 days. C, left, immunofluorescence analysis of HuH1 and HuH7 cells stained with anti–active caspase 3 antibodies. Cells were cultured in 1% FBS DMEM with OSM (100 ng/mL), 5-FU (2 μg/mL), OSM (100 ng/mL) and 5-FU (2 μg/mL), or PBS control for 3 days. Right, bar graphs indicating the percentages of active caspase 3–positive cells.

Noticeably, the combination of OSM and 5-FU effectively suppressed cell proliferation in HuH1 and HuH7 cells (Fig. 4A). We further investigated the effects of OSM and 5-FU on apoptosis, evaluated by Annexin V binding to cell membranes and the activation of caspase 3 (Fig. 4B and C). Although OSM treatment alone had a small effect on the induction of apoptosis, 5-FU treatment induced Annexin V^+ and activated caspase 3^+ cells more than in the control. The

combination of OSM and 5-FU most strongly induced apoptosis in both HuH1 and HuH7 cells with statistical significance.

Finally, we investigated the effect of OSM on EpCAM+ HCC *in vivo* using a primary HCC specimen and cell lines. Single-cell suspensions from primary EpCAM+ HCC cells (1×10^6 cells) were injected into 6-week-old male NOD/SCID mice, and these cells formed subcutaneous tumors 48 days after transplantation. Subsequently, 50 μL of PBS, OSM (2 μg/tumor), 5-FU (250 μg/tumor), or OSM (2 μg/tumor) and 5-FU (250 μg/tumor) solution were injected directly into each tumor twice a week. Although OSM treatment alone showed weak tumor-suppressive effects, the changes in tumor size showed no significant difference compared with controls (Fig. 5A). Similarly, 5-FU treatment alone showed limited tumor-suppressive effects. However, the combination of OSM with 5-FU showed a marked inhibition of tumor growth compared with PBS control or 5-FU alone ($P = 0.02$ and 0.05, respectively). Immunohistochemical analysis of xenografted tumors showed that OSM treatment decreased the number of EpCAM+ or CK19+ cells and increased CYP3A4+ cells *in vivo* (Supplementary Fig. S3A and B). FACS analysis of xenografted tumors further confirmed the decrease of EpCAM+ cell population by OSM treatment *in vivo* (Supplementary Fig. S3C). Immunohistochemical analysis revealed that the combination of OSM with 5-FU strongly induced the activation of caspase 3 compared with PBS control, OSM, or 5-FU (Fig. 5B). Taken together, these data suggest that hepatocytic differentiation of EpCAM+ HCC cells induced by OSM was the most effective for inhibition of tumor growth *in vivo* when the conventional chemotherapeutic agent 5-FU was coadministered.

Discussion

A growing body of evidence suggests that there are similarities between normal stem cells and CSCs in terms of self-renewal programs (29). We have recently reported that Wnt/β-catenin signaling augments self-renewal and inhibits the differentiation of EpCAM+ liver CSCs (18). In the present study, we have shown that the OSM-OSMR signaling pathway is maintained in HCCs with stem/progenitor cell features. OSM induces hepatocytic differentiation and activates cell division in dormant EpCAM+ liver CSCs (Fig. 5C). Furthermore, we have shown that the combination of OSM and 5-FU effectively inhibits tumor cell growth, revealing the importance of targeting both CSCs and non-CSCs for eradication of the tumor.

OSM is a pleiotropic cytokine that belongs to the IL-6 family which includes IL-6, IL-11, and leukemia-inhibitory factor. These cytokines share the gp130 receptor subunit as a common signal transducer, and activate Janus tyrosine kinases and the STAT3 pathway. However, gp130 forms a heterodimer with a unique partner such as the IL-6 receptor, leukemia-inhibitory factor receptor, or OSMR, thus transducing a certain signaling uniquely induced by each cytokine (30). Of note, OSM is known to activate hepatocytic differentiation programs in hepatoblasts in an OSMR-specific manner (27), and our data showed that OSM could induce hepatocytic differentiation and active cell proliferation in EpCAM+ HCC through OSMR signaling.

OSMR is expressed in hepatoblasts in the fetal liver (26). We have found that OSMR is frequently expressed in normal hepatic progenitors but is rarely detected in hepatocytes in adult livers. Interestingly, OSMR+ HCC was characterized by

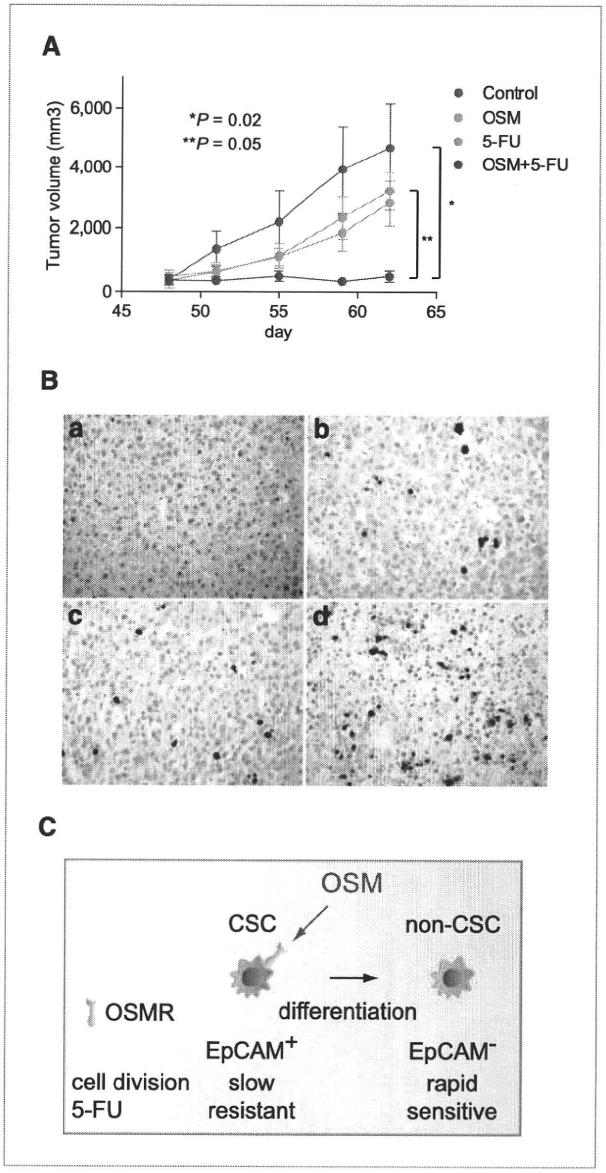

Figure 5. A, effect of PBS, OSM, 5-FU, and OSM plus 5-FU injections on the growth of primary EpCAM+ AFP+ HCC xenograft tumors in NOD/SCID mice ($n = 4$ in each group). Intratumoral injection of 50 μL of PBS, OSM (2 μg/tumor), 5-FU (250 μg/tumor), or OSM (2 μg/tumor) and 5-FU (250 μg/tumor) was initiated 48 days after transplantation, twice per week. B, representative images of activated caspase 3 staining of xenograft tumors in each treatment group (a, PBS; b, OSM; c, 5-FU; and d, OSM and 5-FU). C, a schematic diagram of the effect of OSM on EpCAM+ liver CSCs. Dormant EpCAM+ liver CSCs with OSMR expression respond to OSM and differentiate into rapidly dividing EpCAM- non-CSCs that are highly sensitive to 5-FU.